

# INFLUENCE OF SUBDIVISION FREQUENCY AND BASE POLYHEDRON ON THE STRUCTURAL EFFICIENCY OF SINGLE-LAYER STEEL GEODESIC DOMES

Jakub Szumieluk, Katarzyna Jeleniewicz✉

Institute of Civil Engineering, Warsaw University of Life Sciences – SGGW, Warsaw, Poland

## ABSTRACT

This paper presents a comparative numerical analysis of single-layer steel geodesic domes with a diameter of 30 m based on a regular icosahedron and a regular octahedron. Division frequencies 2 V, 4 V, 8 V, and 16 V were analysed using a Class I grid. The study assumes that increasing the subdivision frequency improves structural performance and that the choice of the base solid affects material efficiency. The results show that higher frequencies reduce bending moments and shift the structural behaviour towards axial forces, which allows smaller cross-sections and lower mass. At 16 V, the icosahedral dome was about 20% lighter than the octahedral one. Domes based on the icosahedron also required fewer unique member lengths and achieved better geometric efficiency.

**Keywords:** geodesic dome, subdivision frequency, icosahedron, octahedron, structural efficiency, parametric modelling

## INTRODUCTION

A geodesic dome is a spatial bar structure with a shape similar to a sphere, constructed from a system of interconnected triangles. The triangular mesh ensures high geometric rigidity and effective, even distribution of loads throughout the structure. Because the elements mainly work under compression and tension, geodesic domes are characterised by high load-bearing capacity and low dead weight. In architecture and construction, these structures are highly valued for their ability to distribute stresses evenly, making them one of the most stable and effective structures available in modern engineering. In addition to geodesic domes, other types of lattice domes are also used, such as lamellar domes, spiral-parallel domes, and Schwedler domes. According to Ramaswamy et al. (2002), assuming the load-bearing capacity of a geodesic dome to be 100%, the load-bearing capacity of a lamellar dome is about 75%, that of a spiral-parallel dome about 50%, and that of a Schwedler dome about 30%.

A key issue in the design of geodesic domes is the shape of the structural grid, in particular the choice of the base solid and the frequency of its wall divisions. As the frequency increases, the number of structural elements increases and the geometry of the dome becomes closer to the surface of a sphere, which has a positive effect on the static performance and spatial rigidity of the structure. At the same time, the increase

in the number of elements leads to greater geometric and technological complexity, which directly affects material consumption and construction difficulty.

Despite the widespread use of geodesic domes in architecture and engineering, previous research has focused mainly on describing the geometry of meshes, division classes – Class I and Class II, and analysing individual mesh division frequencies (Peng, 2016; Szmit, 2017; Bysiec et al., 2024). The literature is dominated by analyses conducted within a single base solid, most often an icosahedron or octahedron, without comparing the two solids. Comparisons of different division classes without a systematic comparison of successive frequencies are also common (Bysiec & Maleska, 2023). There is a lack of studies that compare, under uniform geometric and loading conditions, the impact of the division frequency and the choice of the base solid (octahedron or icosahedron) on the static performance, material efficiency, and functional properties of geodesic domes.

The aim of this article is to conduct a comparative analysis of geodesic domes based on a regular icosahedron and a regular octahedron for division frequencies of 2 V, 4 V, 8 V and 16 V, using a Class I grid division. Only single-layer domes with a uniform diameter of 30 m, designed under identical load conditions, were analysed. The scope of the research includes a comparison of geometric and structural parameters, such as the number of bar elements and nodes, bar lengths, the total length of structural elements, and the dome weight, after selecting cross-sections that meet the requirements for ultimate and serviceability limit states.

The research hypothesis assumes that an increase in the division frequency leads to greater spatial rigidity of the structure and a more even distribution of forces, at the expense of increased element count and material consumption. At the same time, it is assumed that domes based on a regular icosahedron have a more favourable ratio of structural efficiency to dead weight than domes based on an octahedron at comparable division frequencies.

The novelty of this study lies in the systematic comparison of geodesic domes based on two fundamental Platonic solids – the regular icosahedron and the regular octahedron – across a wide range of subdivision frequencies from 2 V to 16 V under identical design assumptions according to Eurocodes.

## HISTORY AND THEORETICAL BACKGROUND

The first structure of this type was designed by Walther Bauersfeld from Carl Zeiss in Jena, in collaboration with Franz Meyer and Friedrich Dischinger (Gáspár & Kis, 2022). The structure was erected on the roof of the Zeiss factory in Jena as an experimental cover for a new planetarium projector. The dome, with a diameter of 16 m, was constructed using the Zeiss–Dywidag system, developed in 1922–1923. This involved spraying a thin layer of concrete onto a steel mesh of about 4,600 rods. In 1925, Dischinger published the first study on dome construction technology, which marked the beginning of its international popularisation (May, 2015). The structure, based on a regular icosahedron, provided high load-bearing capacity with low dead weight – about 39.7 t, of which 3.5 t was steel and 36.2 t was concrete (Peseke et al., 2015). The Zeiss–Dywidag system was one of the first applications of a thin-walled reinforced concrete shell with a geodesic structure in history. The introduction of this technology was groundbreaking – it allowed the creation of large, lightweight, and self-supporting dome structures without the need for internal supports (Hasançebi et al., 2010).

The Bauersfeld and Dischinger method became the prototype for modern geodesic domes, which were developed and popularised by Richard Buckminster Fuller in the 1950s. He opened a new chapter in structural design, in which material efficiency and structural strength became key elements (Fuller, 1982). Fuller emphasised the importance of domes in green building, guided by the principle of ‘doing as much as possible with as little as possible’ (Krausse & Lichtenstein, 1999). This American visionary was guided by synergetic thinking about construction, understood as treating a building as a whole rather than improving selected parameters (Sadowski, 2020). He questioned the idea of building in a Cartesian system, advocating

systems based on the principles of geometry observed in nature, including spherical structures. The geometric system he proposed is based on a modular grid of equilateral triangles, whose  $60^\circ$  angles form the most stable and effective connection system in a plane. As Fuller emphasises, this configuration ‘corresponds to the complex coordination of the most economical and convenient structural interconnections in nature’ (Fuller, 1982).

In his analysis of triangular structures, Fuller points out that nature operates with only three basic spatial arrangements constructed exclusively from equilateral triangles. These are: the tetrahedron, the octahedron, and the icosahedron – the only solids in which triangles can close around a vertex and create a stable, three-dimensional form. In a tetrahedron, three triangles meet at the vertex, in an octahedron four, and in an icosahedron five. Six triangles are no longer able to form a spatial solid, leading only to a flat arrangement. Fuller refers to these forms as omnisymmetric structures, understood as arrangements with complete symmetry at each node, in which the local environment of each vertex remains identical in all directions, and omnitriangulated, meaning that the entire geometry of the solid – all walls, divisions, and partitions – is constructed exclusively from equilateral triangles (Fuller, 1997). Such complete and uniform triangulation makes the structure geometrically stable. This is due to the even distribution of elements in different directions. The repeatability of the arrangement of angles and edges throughout the solid further enhances this stability. The three solids mentioned above perform different functions in Fuller’s geometry. The tetrahedron is the smallest but strongest in terms of volume per unit – it has the most structural elements in relation to its size. The octahedron occupies an intermediate position, while the icosahedron, although relatively the weakest, provides the most volume with the least amount of material. Fuller describes this using the concept of ‘structural quantum’: one quantum corresponds to six edges of a tetrahedron. A tetrahedron requires one such quantum, an octahedron two, and an icosahedron five, but at the same time it is the icosahedron that provides the greatest ‘volume efficiency’ because more than three and a half units of volume are obtained from one structural unit. This reasoning leads Fuller to conclude that the icosahedron is the most economical choice as the basis for a spherical structure: it maintains geometric stability while offering the most space with the fewest elements (Fuller, 1997).

Therefore, in his patent for a geodesic dome, he decided to use the Platonic solid with the largest number of faces – a regular icosahedron. This solid, consisting of 20 equilateral triangles, most closely approximates the shape of a sphere among all regular solids. Fuller projects the geometry of the icosahedron onto the surface of a sphere, transforming its flat triangular faces into spherical triangles whose edges run along the arcs of great circles. The result is a so-called spherical icosahedron – an icosahedron mapped onto a sphere, in which each of the 20 triangles is now an equilateral spherical triangle. The next key step is to divide each triangle’s edges into equal segments. This division, called the grid frequency, determines the grid’s density: the more divisions there are, the closer the dome’s shape approaches a smooth sphere. After dividing the edges, the division points are connected by great-circle arcs that intersect to form a complex grid of small triangles. The resulting nodes of this grid become the connection points for straight structural rods, which form a system corresponding to the chords of great circles. This creates a spherical three-dimensional triangular structure – the geodesic dome (Fuller, 1954). The design of the geodesic dome has not changed significantly since its inception in the mid-20th century. It has retained its original conceptual basis: to cover as much space as possible with minimal use of building materials, while maintaining the lightness of the structure and high spatial rigidity (Kurta & Zemlyansky, 2016). These characteristics have ensured the continued relevance of geodesic domes in modern structural engineering and architectural design.

## GEOMETRY AND STRUCTURAL-MATERIAL CONSIDERATIONS

An important issue in the design of geodesic domes is the method of dividing their structural grid and the selection of an appropriate division frequency. In the case of large-diameter domes, the use of regular

polyhedrons as a basis leads to excessive slenderness of the bar elements. This increases the structure's susceptibility to buckling and requires the use of cross-sections with significantly larger diameters. To improve the structure's performance, the walls are divided into smaller triangles, referred to as the dome frequency.

The subdivision frequency, denoted by the letter  $v$ , refers to the number of equal segments into which the edge of the base triangle is divided. For example, a frequency of 2  $V$  corresponds to the division of the edge into two equal segments, while a frequency of 3  $V$  corresponds to the division into three equal segments. As the subdivision frequency increases, the number of structural elements increases and the geometry of the dome closely approximates the shape of a sphere, which has a positive effect on its static performance (Kubik & Augarde, 2009). The differences between the Class I, Class II, and Class III divisions for successive subdivision frequencies are illustrated in Figure 1.

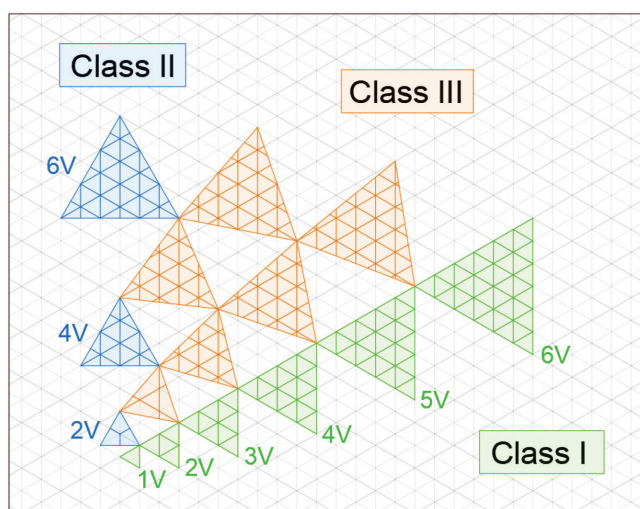


**Fig. 1.** Division of the base triangle into Class I, Class II, and Class III for frequencies ranging from 1  $V$  to 6  $V$

Source: own work.

The literature on the subject distinguishes three basic classes of geodesic dome grid division, referred to as Class I, Class II, and Class III. In Class I division, the lines of the lattice grid run parallel to the edges of the base triangles, and each edge is divided into any number of equal segments. As a result, three families of lines parallel to each edge of the triangle are formed, leading to a regular division of its surface (Fuliński, 1973; Mirski, 1992).

In Class II division, the edges of the base triangle are divided into  $n$  equal parts, after which the dividing lines are drawn parallel to the height of the triangle. These lines pass through the vertex and the centre of the opposite edge. This means that they are parallel to the bisectors of the triangle's angles and at the same time perpendicular to its base (Szmit, 2017). Class III division is also based on dividing the edges of the base triangle into  $n$  equal parts. In this method, additional families of lines parallel to the straight line passing through the triangle's apex and a selected point on the opposite edge are introduced. This point is neither the apex nor the centre of the edge. This results in a grid with mixed geometry, combining the features of Class I and Class II divisions. Due to its greater geometric complexity and more difficult construction analysis, Class III division is rarely used in practice (Fuliński, 1973; Mirski, 1992).

Comparative analyses indicate that dividing the mesh according to the Class I method is more advantageous for numerical modelling and structural performance. This mesh is more regular, which facilitates the creation of computational models and the grouping of bar elements. In the case of Class II division, it is necessary to account for node displacements, which increases the number of member groups and may lead to difficulties during model generation and structure assembly. Domes based on Class I division also exhibit a more even distribution of axial forces and greater stiffness in the vertical direction. In this case, transferring loads to the supports is more advantageous, thereby promoting a more economical foundation design (Bysiec et al., 2024).

The possibility of using a given frequency depends on the grid division class. In the case of Class I division, both even and odd frequency values are acceptable. This division creates a geometry in which the triangle edges lie on the sphere's great circles, facilitating the design of hemispherical domes and the creation of connections in a single plane. In a Class II division, achieving this effect is much more difficult, but the advantage of this solution is that there are fewer different bar lengths, which simplifies their production and assembly. For this reason, Class II division can only be used for even frequency values such as 2 V, 4 V or 6 V (Kubik & Augarde, 2009).

The geometric solutions used in geodesic domes are closely tied to the materials available in a given era. Changes in the way the structural grid is formed and an increase in the division frequency lead to different requirements in terms of the strength and stiffness of the rod elements. For this reason, selecting appropriate construction materials is an important consideration in the design of geodesic domes.

The first material used in the construction of a geodesic dome was reinforced concrete, employed in 1926 for the Zeiss-Planetarium in Jena. The dome was made of steel bars with an  $8 \times 20$  mm cross-section, covered with a thin layer of sprayed concrete that protected the steel elements from corrosion and fire (Peseke et al., 2015; Martínez Martínez et al., 2018). The solution used was innovative for its time, but advances in materials and computational technology later enabled reinforced concrete to be replaced by lighter, more durable materials. In 1954, Fuller patented a dome made of aluminium tubes made of 61ST alloy, corresponding to modern 6061-T6 aluminium (European Committee for Standardization [CEN], 2016; CEN, 2017). The covering was a thin plastic coating, thanks to which the structure with a diameter of 12 m weighed only 517 kg, which was over 76 times lighter than the reinforced concrete dome in Jena, which weighed about 39.7 t. Despite its significantly lower weight, Fuller's structure withstood winds of  $240 \text{ km} \cdot \text{h}^{-1}$  (Fuller, 1954). Lightness, strength, and ease of assembly made aluminium and plastics the basis for the further development of geodesic dome structures. Today, reinforced concrete has been almost completely replaced by steel, aluminium, glued laminated timber, and polymer composites, which combine high load-bearing capacity with low weight and allow for the construction of large spans (Pastukh et al., 2021).

Steel is one of the most commonly used materials in geodesic dome structures. Its high tensile and compressive strength, easy availability and variety of shapes make it suitable for use in both small and large structures. In structural steels used in this type of construction, the yield strength is usually between 235 MPa and 420 MPa (Peng, 2016; Bysiec et al., 2024).

In the case of geodesic domes, where bars work in many directions and at different angles, closed profiles work best, as they provide greater torsional rigidity and even distribution of axial stresses across the cross-section (Talaslioglu, 2019). Thanks to these properties, the entire structure remains stable and works in a predictable manner. When comparing different types of closed sections – circular CHS, rectangular RHS, and square SHS – the circular section proves to be the most effective. With the same cross-sectional area, a circular tube carries greater loads than the other two types, as confirmed by both theoretical calculations and the results of tests on domes with different division frequencies (Shrivastava & Pendharkar, 2021). The use of circular cross-sections reduces the weight of the elements while maintaining the required strength parameters, which is particularly important in structures consisting of thousands of bars. In addition, properly

protected steel, for example by galvanising or painting, is resistant to corrosion and degradation under the influence of environmental factors (Florez et al., 2021). As a result, it combines high durability, resistance, and versatility of application, remaining one of the most frequently chosen materials in spatial structures such as geodesic domes.

The relationship between the geometry of the dome grid, the frequency of division, and the material properties of the rod elements is a key aspect of geodesic dome design. The appropriate selection of geometric and material parameters allows for the creation of a structure with high spatial rigidity, even force distribution, and optimal material consumption.

## MATERIAL AND METHODS

Designing geodesic domes in a parametric environment enables effective shaping of the structure's geometry based on the adopted design parameters. Unlike classic geometric modelling, the structure's form is not defined directly but is described using a set of mathematical relationships and parameters that control its shape. This approach allows for quick modification of the dome geometry, including changes to the division frequency, mesh class and base solid, without the need to rebuild the model manually.

The process of generating geodesic domes was carried out in the Rhinoceros 3D environment, version Rhino 8 SR25 (8.25.25328.11001). The Grasshopper algorithmic editor was used to develop a graphical script. The script was created using standard Grasshopper tools and external plug-ins that extend its functionality: Weaverbird 0.9.0.1, Kangaroo 2.42, LunchBox 2025.5.5.0, AutoGraph 1.2, and EleFront 5.1.8. The tools used enabled the generation of geodesic dome geometry from Platonic solids and their subsequent parametric modification.

Eight geodesic domes with a uniform radius of 15 m were generated in the computing environment – four based on a regular icosahedron and four based on a regular octahedron. Each group of domes was characterised by a different mesh division frequency: 2 V, 4 V, 8 V, and 16 V. In all cases, Class I division was used.

The process of generating a geodesic dome began with the construction of a Platonic solid, a regular icosahedron. Next, at the same geometric centre point, a sphere (Fig. 2) with a radius equal to the radius of the icosahedron was defined, serving as a reference surface for further operations. In the next stage, the lower half of the Platonic solid was removed, yielding a geometry resembling a geodesic dome.

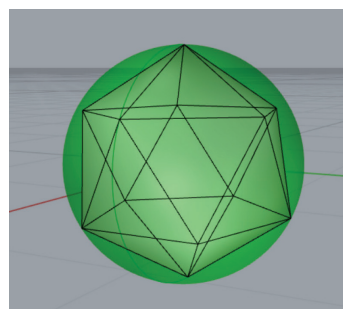


**Fig. 2.** Sphere inscribed in an icosahedron

Source: own work.

The edges of the icosahedron were then iteratively divided into 2, 4, 8 or 16 equal parts, allowing for different frequencies of the geodesic mesh. The newly created division points were transferred radially, along lines emanating from the geometric centre of the original figure, onto the surface of the sphere. The newly created points were connected according to the triangulation principle derived from the initial solid, resulting in a dense triangular spatial structure with a spherical shape (Fig. 3). The process was repeated for a regular octahedron.

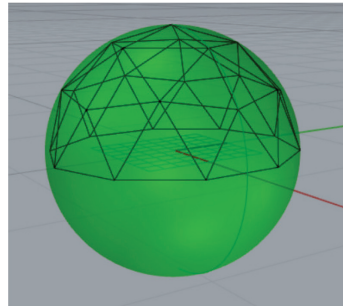


**Fig. 3.** Newly created points transferred to the surface of the sphere

Source: own work.

The use of parametric design tools allowed precise definition of geometric relationships between the structural elements and full control over the geometric parameters of the analysed domes. A graphical script in the Grasshopper environment enabled easy modification via sliders for parameters such as the radius, height, frequency of geodesic dome division, and the selection of the solid's base, as shown in Figure 4.

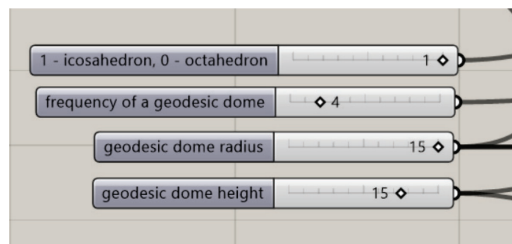


**Fig. 4.** Fragment of the author's graphic script generating geodesic domes

Source: own work.

Eight geodesic dome grids generated in Grasshopper (Figs 5 and 6) were then exported to Autodesk Robot Structural Analysis Professional 2023 for static and strength analysis and selection of structural element cross-sections. Each dome was modelled as a spatial bar system corresponding to the geometry generated in the parametric environment. All members were modelled using 3D beam elements with six degrees of freedom per node. Hinged connections between members were assumed, allowing free rotation at the nodes and ensuring axial force-dominated structural behaviour typical for geodesic domes. Buckling lengths of members were assumed equal to their actual lengths, corresponding to pinned connections between elements and preventing additional rotational restraint.

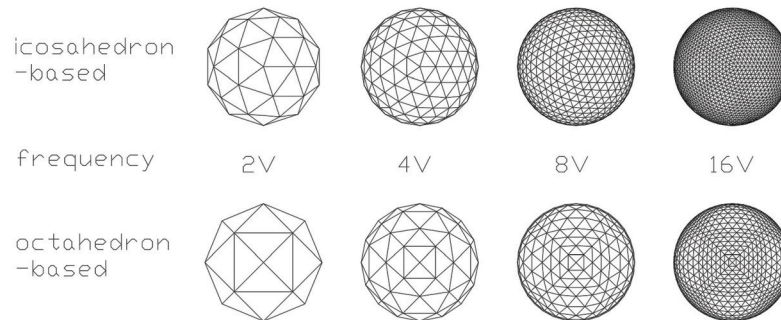


**Fig. 5.** Comparison of geodesic grid geometries generated in Rhinoceros 3D based on icosahedron and octahedron polyhedra with varying subdivision frequencies – top view

Source: own work.

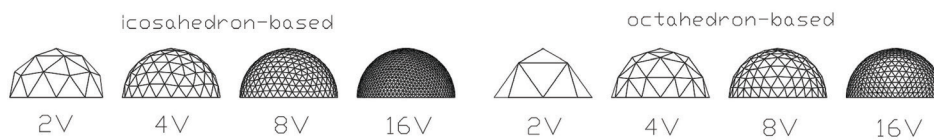


**Fig. 6.** Comparison of geodesic grid geometries generated in Rhinoceros 3D based on icosahedron and octahedron polyhedra with varying subdivision frequencies – side view

Source: own work.

The computational models assumed supports in the form of fixed points located at each node of the dome base. This assumption corresponds to the presence of a stiff reinforced concrete ring beam typically used in real dome structures. The fully fixed support model was adopted to ensure consistent comparative conditions for all analysed variants and to eliminate the influence of foundation flexibility on structural performance. The loads were transferred to the supporting structure indirectly through the cladding assigned to the dome surface, representing the covering layer (Fig. 7). This approach enabled a realistic representation of the manner in which loads are transferred from the covering to the load-bearing structure.

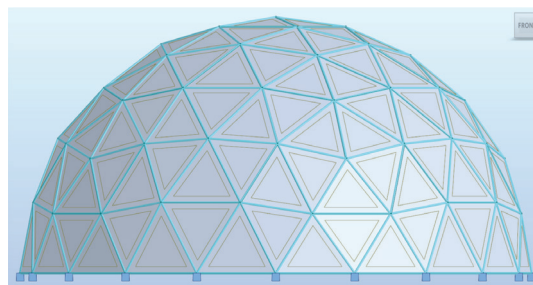


**Fig. 7.** Numerical model of a geodesic dome developed using a regular icosahedron with subdivision frequency of 4 V. The model displays the arrangement of structural members, claddings, and supports

Source: own work.

The structure was subjected to dead loads, snow loads, and wind actions, determined in accordance with applicable European standards (Polski Komitet Normalizacyjny [PKN], 2004a; PKN, 2004b; PKN, 2005a; PKN, 2005b).

The structural dead load consists of circular hollow section steel members of grade S235. These sections were selected using Autodesk Robot Structural Analysis 2023 software to satisfy both ultimate limit state and serviceability limit state requirements. The dimensions of the circular tubes were determined individually for each dome.

The non-structural permanent load was established as follows: the roofing system was assumed to be a PIR sandwich panel with a thermal transmittance coefficient of  $U = 0.15 \text{ W} \cdot \text{m}^{-2} \cdot \text{K}^{-1}$ , which satisfies current national regulatory requirements for roof structures (Obwieszczenie Ministra Rozwoju i Technologii z dnia 15 kwietnia 2022 r.). The total permanent non-structural load of  $0.34 \text{ kN} \cdot \text{m}^{-2}$  (Fig. 8) consists of  $0.14 \text{ kN} \cdot \text{m}^{-2}$  corresponding to the roofing system, based on manufacturer data (Blachy Pruszyński, n.d.), and  $0.20 \text{ kN} \cdot \text{m}^{-2}$  representing technical installations and service equipment (PKN, 2004b).

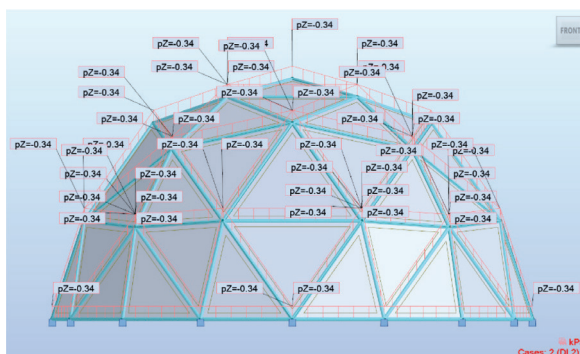


**Fig. 8.** Numerical model of a 4 V octahedron-based geodesic dome showing structural members, cladding and supports under permanent load

Source: own work.

Snow loads were calculated in accordance with the standard PN-EN 1991-1-3. The designed geodesic dome is in Tarczyn, Poland, at an altitude of 140 m above sea level. This location is classified as snow load zone II according to PN-EN 1991-1-3 guidelines. Three snow load patterns were analysed, corresponding to different possibilities of its uneven distribution on the dome surface – a uniform snow load of  $0.72 \text{ kN} \cdot \text{m}^{-2}$  and two asymmetrical cases, with  $0.90 \text{ kN} \cdot \text{m}^{-2}$  on one half of the dome and  $0.45 \text{ kN} \cdot \text{m}^{-2}$  on the other.

Wind actions were determined based on PN-EN 1991-1-4. The location of Tarczyn belongs to wind zone 1 and terrain category I. For the given site and dome parameters, the fundamental wind velocity is  $25.41 \text{ m} \cdot \text{s}^{-1}$ . The wind loads were generated automatically in the Autodesk Robot Structural Analysis 2023 software for eight different wind directions: the four cardinal directions – north, south, east, west – and the four intermediate directions.

The adopted modelling assumptions and load application strategy are consistent with previous studies on wind and structure interaction in geodesic domes (Jeleniewicz et al., 2025). Load combinations were created automatically in accordance with Eurocode 1 for ultimate and serviceability limit states.

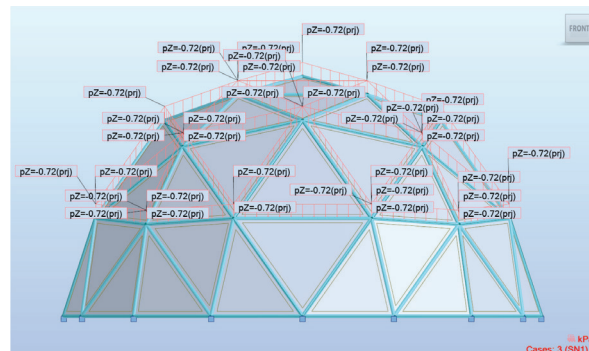


**Fig. 9.** Numerical model of a 4 V octahedron-based geodesic dome showing structural members, cladding and supports under uniformly distributed snow load

Source: own work.

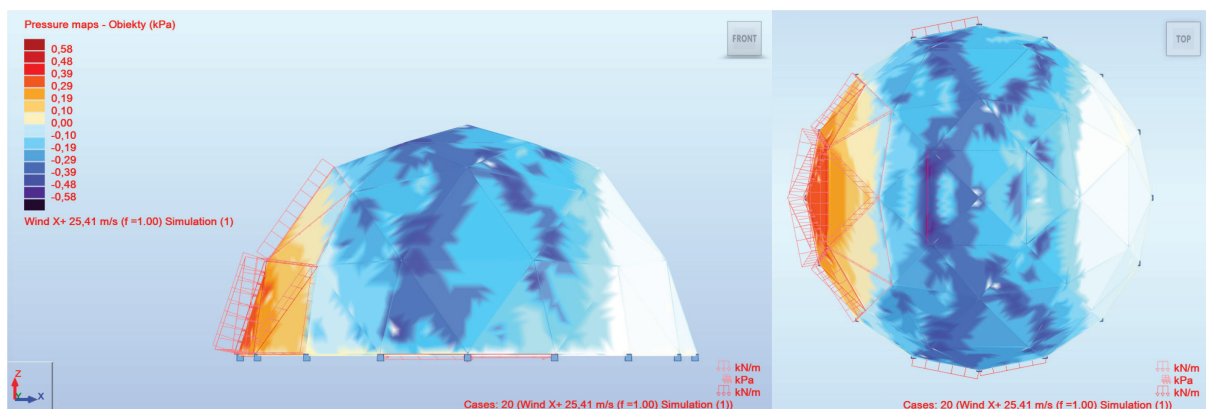


**Fig. 10.** Numerical model of a 4 V octahedron-based geodesic dome showing structural members, supports and an automatically generated wind load case

Source: own work.

The static analysis made it possible to determine the distribution of internal forces in the bars, normal stresses, node displacements, and support reactions. Based on the results obtained, the cross-sections of the structural elements were selected. The selection of cross-sections was carried out in Autodesk Robot Structural Analysis Professional 2023 using a catalogue of Polish profiles. S235 steel round tubes were used, which, due to their geometry, most effectively transfer axial loads in geodesic dome structures (Shrivastava & Pendharkar, 2021).

The selected cross-section had to meet the standard requirements for serviceability limit states. In accordance with Eurocode 3 and the relevant national annexes (PKN, 2006a; PKN, 2006b), it was assumed that the maximum deflection of structural elements should not exceed  $L/250$ , while the horizontal displacement of structural nodes was limited to  $H/150$ . In addition, the load-bearing capacity conditions in the ultimate limit states were checked, including the stability condition of bar elements.

In the first stage, profiles with the smallest available diameter and the greatest possible wall thickness were analysed, meeting the requirements for ultimate limit states and serviceability limit states. Next, profiles

with larger diameters were considered, each time assuming a minimum wall thickness greater than 3 mm, which allowed the limit states of load-bearing capacity and serviceability to be met. In the following steps, intermediate cross-sections were analysed, modifying the combinations of diameter and wall thickness in order to obtain cross-sections that met the standard requirements.

The cross-section was selected for the entire dome, assuming the same cross-section for all structural bars. This assumption enabled full standardisation of the elements and simplified the prefabrication and assembly process. From among all cross-sections meeting the limit state requirements, the one with the smallest cross-sectional area was selected. The research approach adopted enabled a direct comparison of the influence of the base solid and the division frequency on the geometric parameters, static behaviour, and material efficiency of the analysed geodesic domes.

## RESULTS

### Comparative analysis – general assumptions

Eight geodesic domes with a diameter of 30 m were the subject of comparative analysis. Four domes were designed on the basis of a regular icosahedron, and four on the basis of a regular octahedron. For both base solids, grid division frequencies of 2 V, 4 V, 8 V, and 16 V were adopted, while maintaining the same division class.

The analysis includes a comparison of geometric parameters, static calculation results, and the weight of the structure after selecting the bar cross-sections.

### Mesh geometry and structural complexity

A summary of the basic geometric parameters of the analysed domes is presented in Table 1. The analysis of geometric parameters showed that an increase in the mesh frequency leads to a significant increase in the number of bars and nodes in both analysed dome types. For a frequency of 2 V, the octahedron-based dome consists of 28 bars and 13 nodes, while the icosahedron-based structure comprises 65 bars and 26 nodes. At the highest frequency analysed, 16 V, the number of elements increases to 1,568 rods in the octahedral dome and 3,880 rods in the icosahedral dome, respectively. These results indicate a significantly greater geometric complexity of meshes based on a solid with a larger number of base faces.

**Table 1.** Geometric and structural parameters of geodesic domes (Class I division grid – 30 m diameter)

Parameter	Base							
	regular octahedron				regular icosahedron			
Division frequency [V]	2	4	8	16	2	4	8	16
Number of members	28	104	400	1,568	65	250	980	3,880
Number of nodes	13	41	145	545	26	91	341	1,321
Number of claddings	16	64	256	1,024	40	160	640	2,560
Average member length [m]	12.99	6.99	3.58	1.80	8.78	4.50	2.26	1.13
Max member length [m]	15.00	8.66	4.52	2.29	9.27	4.87	2.47	1.24
Min member length [m]	11.48	5.85	2.82	1.37	8.20	4.14	2.03	1.00
Sum of member length [m]	363.68	726.96	1,430.64	2,825.52	570.45	1,124.20	2,215.98	4,393.30
Degree of strut length variation	2	5	17	41	2	5	13	18
Sum of surface of external panels [m <sup>2</sup> ]	1,172.00	1,344.93	1,395.86	1,409.21	1,312.42	1,387.11	1,406.98	1,412.03
Interior volume [m <sup>3</sup> ]	4,965.99	6,442.42	6,907.98	7,029.97	6,063.70	6,823.71	7,009.82	7,055.73
Surface-to-volume ratio	0.2360	0.2088	0.2021	0.2005	0.2164	0.2033	0.2007	0.2001

Source: own work.

The densification of the mesh is accompanied by a systematic reduction in the length of the rod elements. The average length of a rod in a dome based on an octahedron decreases from 12.99 m for 2 V to 1.80 m for 16 V. In the case of a 20-sided dome, this reduction is even more pronounced, ranging from 8.78 m to 1.13 m. It has been observed that domes based on a 20-sided shape are characterised by a denser and more uniform mesh even at lower frequencies.

An important issue from the construction perspective is variation in bar lengths. Despite having more elements, 20-sided domes require fewer unique bar lengths. In the analysed range, the number of bar types ranges from 2 to 18, while in octagonal domes it increases from 2 to 41. A smaller number of different element lengths simplifies the prefabrication process and assembly logistics, which has direct practical significance.

The results obtained clearly indicate that domes based on an icosahedron, even at lower division frequencies, are characterised by a more homogeneous and geometrically efficient mesh than structures based on an octahedron. Table 1 provides a concise overview of the fundamental geometric parameters of the analysed domes.

### **Surface area, volume and geometric efficiency of domes**

As the division frequency increases, the external surface area and volume of both dome types gradually approach those of a hemisphere with a radius of 15 m. However, this process is faster in the case of structures based on an icosahedron. Already at a frequency of 2 V, the icosahedral dome achieves an external surface area of 1,312.42 m<sup>2</sup> and a volume of 6,063.70 m<sup>3</sup>, while the octahedral model has a surface area of 1,172.00 m<sup>2</sup> and a volume of 4,965.99 m<sup>3</sup>. This means a better approximation of the spherical form at the same division frequency in favour of the icosahedral dome.

At a frequency of 16 V, the differences between the two structures are significantly reduced, and the domes' volume fluctuates around 7,050 m<sup>3</sup>. As the mesh becomes denser, the surface-to-volume ratio, an important indicator of geometric efficiency, decreases. The lowest values of this parameter were obtained at a frequency of 16 V, with 0.2005 for the octahedral dome and 0.2001 for the icosahedral dome.

A lower surface-to-volume ratio means less external surface area per unit of building volume, which helps reduce heat loss. Across the entire range of frequencies analysed, an icosahedron shows more favourable values for this ratio. This demonstrates its higher geometric efficiency and, indirectly, its higher energy efficiency compared to structures based on an octahedron.

The results clearly indicate that icosahedron-based domes achieve a more uniform mesh and better geometric efficiency at lower division frequencies, while octahedron-based domes remain structurally simpler but less material-efficient.

### **Static analysis**

The extreme values of internal forces and the degree of stress on the most heavily loaded elements are summarised in Table 2. The analysis carried out in Autodesk Robot Structural Analysis 2023 made it possible to determine the extreme values of internal forces and the degree of stress on the most heavily loaded bars in each of the eight domes analysed. The results indicate that both the choice of the base solid and the frequency of the mesh division have a significant impact on the static behaviour of critical elements. In structures with a low division frequency, especially in octahedron-based domes, the most stressed bars carry significant bending moments, with a maximum value of 218.61 kNm. This type of structure requires the use of profiles with high stiffness and larger cross-sections.

With an increase in the division frequency to 16 V, a significant decrease in bending moments in the most heavily loaded elements was observed. This leads to a change in the structure's operational nature and a transition to a state dominated by axial forces, which is beneficial from the point of view of material optimisation.

**Table 2.** Extremal internal forces and utilisation ratios for the most loaded members (Class I division grid – 30 m diameter)

Parameter	Base							
	regular octahedron				regular icosahedron			
Division frequency [V]	2	4	8	16	2	4	8	16
Cross-section type – CHS	508 × 6	244.5 × 5	127 × 4	54 × 3.2	323.9 × 5	139.7 × 4	63.5 × 3.2	26.9 × 3.6
Ultimate limit state utilisation ratio	0.81	0.63	0.53	0.79	0.52	0.64	0.76	0.99
Serviceability limit state utilisation ratio	0.98	0.94	0.83	0.92	0.79	0.92	0.87	0.83
Maximum axial forces [kN]	143.65	95.75	49.33	25.11	113.11	61.00	29.42	15.24
Minimum axial forces [kN]	-35.53	-85.03	-54.87	-29.08	-79.74	-68.25	-35.92	-19.53
Maximum shear forces [kN]	45.29	13.70	4.14	1.05	20.54	5.52	1.38	0.35
Minimum shear forces [kN]	-45.29	-13.70	-4.14	-1.05	-20.54	-5.52	-1.38	-0.35
Maximum bending moments [kNm]	218.61	36.15	6.13	0.77	61.90	8.71	1.12	0.14
Minimum bending moments [kNm]	-8.84	-2.79	-0.74	-0.12	-4.06	-0.90	-0.17	-0.03
Maximum torsional moments [kNm]	23.92	9.22	1.83	0.22	13.50	2.42	0.34	0.04
Minimum torsional moments [kNm]	-36.37	-11.29	-1.53	-0.23	-13.57	-2.40	-0.34	-0.04

Source: own work.

In most of the analysed models, the selection of cross-sections was determined by the serviceability limit state, which was the first to reach values close to the permissible ones. This indicates that, under the assumptions made, S235 steel was the optimal solution for ensuring the required structural rigidity. The exception was the dome with a frequency of 16 V based on an icosahedron, in which the decisive factor was the ultimate limit state, reaching a value close to unity.

Further verification of this variant using higher-grade S355 steel confirmed the possibility of additional structural optimisation. The use of higher-strength steel allowed the profile wall thickness to be reduced from 3.6 mm to 3.2 mm while maintaining the same outer diameter of 26.9 mm. This measure reduced the stress level at the ultimate load capacity to 0.92 and at the same time improved the balance of the structure in terms of usability. These results indicate that at high-division frequencies, when the structure becomes extremely light, the use of higher-strength steel is an effective way to reduce the dead weight without the risk of exceeding the limit states in the most heavily loaded elements.

Increasing division frequency shifts the structural behaviour towards a predominantly axial force system, enabling significant reduction of cross-sections and total structural mass.

### Structure weight

The total masses of the structures are presented in Table 3. Analysis of the total mass of the tested structures showed a clear downward trend with increasing mesh frequency. This phenomenon results directly from the possibility of gradually reducing the cross-sections of the bars, made possible by a more favourable distribution of internal forces in denser meshes. In the case of octahedron-based domes, the total mass decreases from 27,017 kg for a frequency of 2 V to 11,365 kg for 16 V. Even greater material efficiency was achieved for structures based on an icosahedron, where the mass of a 2 V dome is 22,443 kg, and for the 16 V variant it drops to 9,148 kg. This means that with the same structure diameter and the highest analysed division frequency, the dome based on an icosahedron is about 20% lighter than the equivalent solution based on an octahedron.

The steel grade used also significantly affects the structure's final weight. For the most effective variant, the 20-sided dome with a frequency of 16 V, replacing S235 steel with S355 steel enabled a further reduction

in the cross-sections of the bars. The cross-sectional area decreased from 264 mm<sup>2</sup> to 238 mm<sup>2</sup>, which translated into a decrease in the unit weight of the element from 2.07 kg·m<sup>-1</sup> to 1.87 kg·m<sup>-1</sup>. On the scale of the entire structure, this resulted in a reduction in total weight of 901 kg, from 9,148 kg to 8,247 kg.

**Table 3.** Comparison of material consumption and unit weights for different dome frequencies (Class I division grid – 30 m diameter)

Parameter	Base							
	regular octahedron				regular icosahedron			
Division frequency [V]	2	4	8	16	2	4	8	16
Cross-section type – CHS	508 × 6	244.5 × 5	127 × 4	54 × 3.2	323.9 × 5	139.7 × 4	63.5 × 3.2	26.9 × 3.6
Cross-sectional area [mm <sup>2</sup> ]	9,462	3,762	1,546	511	5,009	1,705	606	264
Unit weight [kg·m <sup>-1</sup> ]	74.29	29.53	12.17	4.01	39.34	13.43	4.76	2.07
Total dome mass [kg]	27,017	21,488	17,432	11,365	22,443	15,118	10,572	9,148

Source: own work.

The results obtained confirm that in structures with a high division frequency, the use of steel with a higher yield strength is an effective method of material optimisation. This allows for a further reduction in the dead weight of the structure while meeting the requirements for load-bearing capacity and serviceability, resulting in the lightest and most effective of the analysed geodesic dome forms.

For the highest analysed frequency (16 V), the icosahedral dome proved about 20% lighter than the corresponding octahedral dome, confirming its superior material efficiency. The results show that both the base solid and the subdivision frequency significantly affect the geometric complexity and material efficiency of geodesic domes. Structures based on an icosahedron demonstrate superior mesh uniformity and higher geometric efficiency across the entire range of analysis.

### Geometric and material efficiency indicators

To quantitatively evaluate the analysed variants, a material efficiency index ( $E_m$ ) was introduced. The index defines the relationship between the dome volume and its structural mass:

$$E_m = \frac{V}{M}. \quad (1)$$

where:

$V$  – volume of the dome [m<sup>3</sup>],

$M$  – mass of the structure [kg].

The analysis of  $E_m$  (Fig. 11) demonstrates that the material efficiency of the structure increases with the frequency of division. It can thus be concluded that a higher mesh density allows for a more favourable volume-to-mass ratio. Throughout the analysed range, an icosahedron achieves higher index values. This finding indicates that it makes better use of construction material.

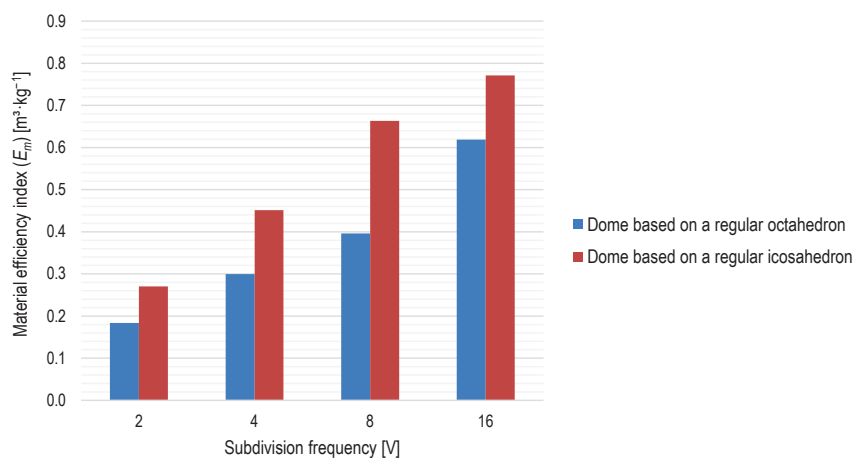


**Fig. 11.** The material efficiency index of geodesic domes based on a regular octahedron and a regular icosahedron

Source: own work.

A direct comparison of masses is shown in Figure 12. As the division frequency increases, the mass of the octahedron-based dome decreases from 27,017 kg to 11,365 kg – a decrease of about 58%, while in the case of the icosahedral dome, it decreases from 22,443 kg to 9,148 kg – a decrease of about 59%. This means that both structures show similar dynamics of mass reduction. At the same time, throughout the entire analysed range, icosahedral domes remain lighter – the difference is about 17% for 2 V and increases to about 20% for 16 V.

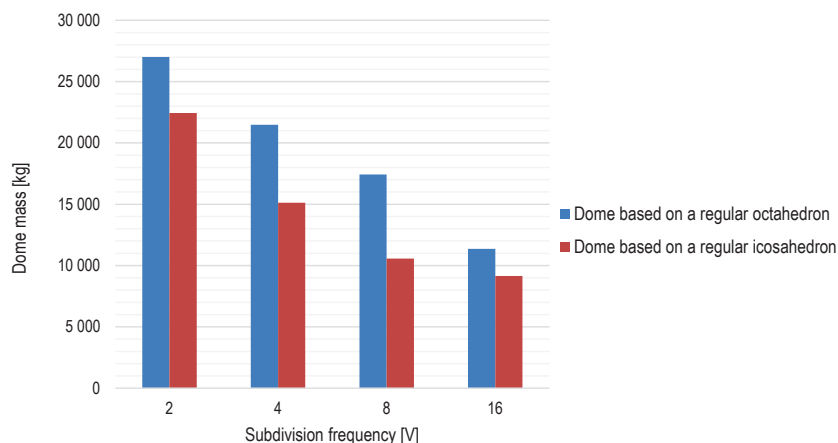


**Fig. 12.** Mass versus subdivision frequency of geodesic domes based on a regular octahedron and a regular icosahedron

Source: own work.

The relationship between mass and the number of bar elements (Fig. 13) confirms that mass reduction is directly related to mesh density. An increase in the number of bars causes the structure to transition to a state of operation dominated by axial forces, which allows for the use of smaller cross-sections and further

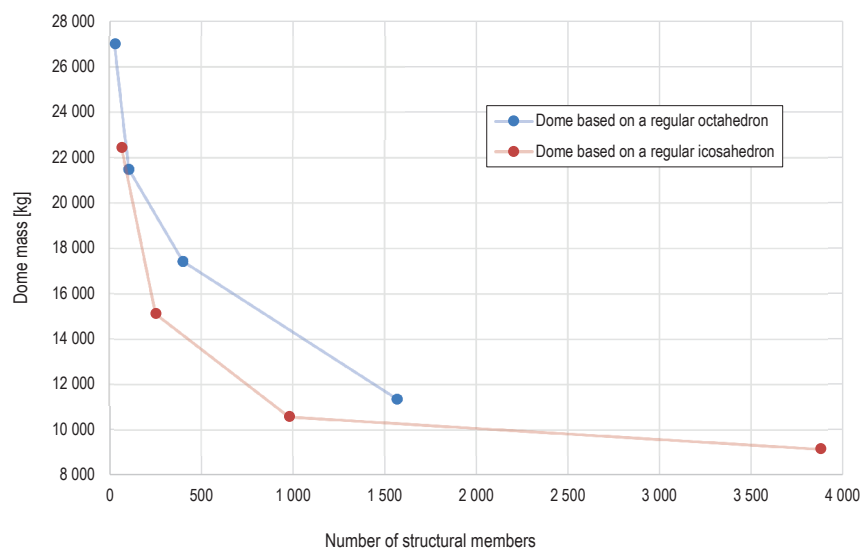


**Fig. 13.** Dome mass versus number of structural members for geodesic domes based on a regular octahedron and a regular icosahedron.

Source: own work.

mass reduction. The results obtained therefore indicate a compromise between weight reduction and increased geometric complexity, with solutions based on an icosahedron providing a more favourable relationship between these two aspects.

## DISCUSSION

The numerical results are consistent with previous studies on geodesic structures. The calculations confirm the assumptions formulated by Fuller, namely that a regular icosahedron is the most effective base shape in terms of uniform stress distribution and material efficiency. The advantage of icosahedron-based domes over octahedron-based solutions is evident in terms of both global stiffness and the uniformity of the rod mesh. These trends are confirmed by analyses carried out in the Autodesk Robot Structural Analysis software and by observations presented by Kenner, who notes less variation in element length and a more even distribution of curvature in icosahedral systems, which limits the formation of local areas of structural weakness (Kenner, 2003).

With increased mesh division frequency, a clear reduction in bending moments in structural elements was observed. This phenomenon indicates a gradual transition of the structure to a state of operation dominated by axial forces. Similar conclusions were drawn by Lendave et al. (2024). In this study, for a dome based on an octahedron with a frequency of 16 V, the maximum bending moment decreased to below 1 kNm, compared to 218.61 kNm for the 2 V variant, clearly confirming the high static efficiency of dense geodesic meshes.

A review of the literature indicates that there are only a limited number of studies comparing the behaviour of geodesic domes based on icosahedrons and octahedrons at high division frequencies, such as 16 V. Most available publications focus on lower frequencies or on the analysis of a single base solid. The comparison carried out in this study shows that the choice of the base solid has a significant impact not only on the uniformity of the rod mesh, but also on the complexity of the structure and its global stiffness. In the analysed variants,

the number of different bar lengths for a dome based on an icosahedron was significantly lower, amounting to 18 types, while for a dome based on an octahedron it reached 41 types. This difference is of direct importance with respect to the prefabrication, transport, and assembly of the structure.

Previous studies have focused mainly on comparing mesh division classes, such as Class I and Class II, often overlooking the influence of the base solid itself and the behaviour of the structure at very high division frequencies (Bysiec et al., 2024). The results of this study indicate that at a frequency of 16 V, the choice between an icosahedron and an octahedron becomes a key factor for the static efficiency and construction complexity of the structure, regardless of the mesh division class adopted.

It should also be noted that studies describe the mathematical and geometric basis for generating geodesic grids for various base solids and frequencies, but most are theoretical and do not include detailed strength analyses (Davis, 2011). These publications provide tools for creating structural geometry but rarely refer to actual load conditions and material optimisation. This work fills this gap by combining geometric analysis with a complete static and strength analysis in accordance with design standards, allowing for a practical assessment of the validity of using specific solutions in large-span geodesic dome engineering structures.

However, it should be emphasised that the presented results are based on a linear static first-order analysis, without accounting for geometric imperfections, material non-linearity, or second-order effects. These factors can significantly affect the actual load-bearing capacity and stability of highly slender bar structures. Studies on ribbed and spatial domes have shown that accounting for geometric imperfections and non-linearities can lead to a significant reduction in the ultimate load-bearing capacity and changes in the structure's behaviour (Jeleniewicz et al., 2024). This means that further research should include nonlinear analyses and an assessment of the sensitivity of structures to geometric imperfections, especially for domes with very high division frequencies and small bar cross-sections.

## CONCLUSIONS

A comparative analysis of eight geodesic dome variants with a 30 m diameter showed that the choice of base solid has a clear impact on structural behaviour and material consumption. Domes based on a regular icosahedron create a more uniform grid than those generated from an octahedron. They require fewer distinct member lengths and better approximate a spherical shape, leading to a more even distribution of internal forces.

Increasing the subdivision frequency from 2 V to 16 V changes how the structure operates. Bending moments decrease, while axial forces become dominant in the most loaded members. This allows reducing the bar cross-sections and the overall structural mass without compromising stiffness or load-bearing capacity. In most analysed cases using S235 steel, the cross-section selection was governed by the serviceability limit state. This shows that in large-span geodesic domes, stiffness and displacement control are more important than the ultimate resistance of individual elements.

For the highest subdivision frequency of 16 V, the governing criterion shifted towards the ultimate limit state. The use of higher strength steel grade S355 allowed a reduction of the total structural mass by about 10%. Despite the larger number of members, domes based on an icosahedron are also easier to prefabricate and assemble due to the lower number of unique bar lengths, equal to 18 compared to 41 in the octahedron-based variant.

On the basis of these findings, some specific design recommendations for engineering practice can be formulated. For large-span structures reaching 30 m, the icosahedron-based 16 V frequency is the most efficient configuration. This model offers an optimal balance between sphere approximation and internal force distribution. When using such high subdivision frequencies, the use of S355 steel is recommended to maximise material efficiency and weight reduction. Designers should also prioritise global stability and stiffness analysis, as serviceability limits often dictate the final cross-sections before the material's strength is even fully utilised.

The high level of standardisation in icosahedron-based grids is a significant advantage over octahedron-based variants, as it simplifies the assembly process and reduces the potential for manual errors during construction.

The study shows that the initial geometry selection is a decisive factor for the overall structural efficiency and technical feasibility. Higher frequency domes involve more nodes and connections, but the benefits of mass reduction and structural uniformity usually outweigh the increased complexity of the grid. Future research should focus on expanding the scope of the analysis to include domes with different diameters, such as 20 m or 50 m. This will help verify if these trends remain consistent across various scales. Additionally, further studies are planned to examine other geometrical configurations and alternative subdivision schemes to provide a more comprehensive comparison of structural efficiency in geodesic systems.

### Acknowledgements

The author acknowledges the support of the Warsaw University of Life Sciences (SGGW) for providing access to computational software used in this study.

### Authors' contributions

Conceptualisation: J.S. and K.J.; methodology: J.S.; validation: J.S. and K.J.; formal analysis: J.S.; investigation: J.S.; resources: J.S. and K.J.; data curation: J.S.; writing – original draft preparation: J.S.; writing – review and editing: K.J.; visualisation: J.S.; supervision: K.J.

All authors have read and agreed to the published version of the manuscript.

### REFERENCES

- Blachy Pruszyński. (n.d.). *PWS-PIR-CH-140 sandwich panel – technical specifications*. <https://pruszynski.com.pl/produkt/plyty-warstwowe/plyty-warstwowe-pirtech/pirtech-chlodnia/pws-pir-ch-140-plyta-warstwowa-scienna-chlodnicza-pianka-poliuretanowa-widoczne-mocowanie/> [accessed: 2.04.2026].
- Bysiec, D., & Maleska, T. (2023). Influence of the mesh structure of geodesic domes on their seismic response in applied directions. *Archives of Civil Engineering*, 69(3), 65–78. <https://doi.org/10.24425/ace.2023.146067>
- Bysiec, D., Jaszczyński, S., & Maleska, T. (2024). Analysis of lightweight structure mesh topology of geodesic domes. *Applied Sciences*, 14(1), 132. <https://doi.org/10.3390/app14010132>
- Davis, T. (2011). *Geodesic domes*. [http://www.domerama.com/wp-content/uploads/2013/01/geodesic\\_dome\\_davis.pdf](http://www.domerama.com/wp-content/uploads/2013/01/geodesic_dome_davis.pdf) [accessed: 2.04.2026].
- European Committee for Standardization [CEN]. (2016). *Aluminium and aluminium alloys. Extruded rod/bar, tube and profiles. Part 2: Mechanical properties (EN 755-2)*.
- European Committee for Standardization [CEN]. (2017). *Aluminium and aluminium alloys. Wrought products. Temper designations (EN 515)*.
- Florez, F., Fernández-de-Córdoba, P., Taborada, J., Castro-Palacio, J. C., Higón-Calvet, J. L., & Pérez-Quiles, M. J. (2021). Passive strategies to improve the comfort conditions in a geodesic dome. *Mathematics*, 9(6), 663. <https://doi.org/10.3390/math9060663>
- Fuliński, J. (1973). *Geometria kratownic powierzchniowych*. Wrocławskie Towarzystwo Naukowe.
- Fuller, R. B. (1954). *Geodesic dome* (U.S. Patent No. 2,682,235). United States Patent and Trademark Office.
- Fuller, R. B. (1982). *Synergetics: Explorations in the geometry of thinking*. Estate of R. Buckminster Fuller.
- Fuller, R. B. (1997). *Synergetics: Explorations in the geometry of thinking* (with E. J. Applewhite). Macmillan Publishing Co.
- Gáspár, O., & Kis, A. É. (2022). Searching for the engineering optimum: Evolution of the topology of the triangulated rebar grid of the Zeiss-Dywidag domes. In *Proceedings of IASS Annual Symposia* (Vol. 2022, No. 10, pp. 1–11). International Association for Shell and Spatial Structures (IASS). <https://www.ingentaconnect.com/contentone/iass/piass/2022/00002022/00000010/art00009> [accessed: 2.04.2026].

- Hasançebi, O., Erdal, F., & Saka, M. P. (2010). Optimum design of geodesic steel domes under code provisions using metaheuristic techniques. *International Journal of Engineering and Applied Sciences*, 2(2), 88–103. <https://izlik.org/JA42ZK55DU> [accessed: 2.04.2026].
- Jeleniewicz, K., Jaworski, J., Żółtowski, M., Uziębło, I., Stefańska, A., & Dixit, S. (2024). Steel ribbed dome structural performance with different node connections and bracing system. *Scientific Reports*, 14(1), 14013. <https://doi.org/10.1038/s41598-024-64811-0>
- Jeleniewicz, K., Szlachetka, O., & Piekarczyk, A. (2025). Kupa geodezyjna kontra wiatr: normy, MES i CFD w nowoczesnym projektowaniu. *Przegląd Budowlany*, 96(6), 167–170. <https://doi.org/10.5604/01.3001.0055.4959>
- Kenner, H. (2003). *Geodesic math and how to use it*. University of California Press [Original work published 1976].
- Krausse, J., & Lichtenstein, C. (Eds.). (1999). *Your private sky: R. Buckminster Fuller. The art of design science*. Lars Müller Publishers.
- Kubik, M., & Augarde, C. (2009). *Structural analysis of geodesic domes* (Final year project). Durham University, School of Engineering.
- Kurta, I., & Zemlyansky, V. (2016). Preconditions for technological development of the construction industry of the North for the arrangement of the mineral complex of the Russian Arctic. *Procedia Engineering*, 165, 1542–1546. <https://doi.org/10.1016/j.proeng.2016.11.891>
- Lendave, K. B., Dhanshetti, P. V., & Patil, S. S. (2024). Class I and Class II subdivision of the 20-meter geodesic dome behavior and analysis using breakdown methods 1 and 2 for various dome frequencies. *Nanotechnology Perceptions*, 20(S1). <https://doi.org/10.62441/nano-ntp.v20is1.2>
- Martínez Martínez, M., Echeverría Valiente, E., García-Rosales González-Fierro, G., & Moreno Gata, K. (2018). The preservation of the architectural heritage of the twentieth century: the laminar structure of reinforced concrete. In C. Gambardella (ed.), *World heritage and knowledge: representation, restoration, redesign, resilience. XVI International Forum "Le Vie dei Mercanti"*. Gangemi Editore.
- May, R. (2015). Shell sellers: The international dissemination of the Zeiss-Dywidag system, 1923–1939. In *Proceedings of the 5th International Congress on Construction History* (Vol. 2, pp. 557–564). <https://gesellschaft.bautechnikgeschichte.org/wp-content/uploads/2015/07/may.pdf> [accessed: 2.04.2026].
- Mirski, J. Z. (1992). Siatki powstałe z przekształceń 8-ścianu foremnego. *Zeszyty Naukowe Akademii Rolniczej we Wrocławiu. Melioracja*, 41(212), 27–39.
- Obwieszczenie Ministra Rozwoju i Technologii z dnia 15 kwietnia 2022 r. w sprawie ogłoszenia jednolitego tekstu rozporządzenia Ministra Infrastruktury w sprawie warunków technicznych, jakim powinny odpowiadać budynki i ich usytuowanie. Dz.U. 2022 poz. 1225. <https://isap.sejm.gov.pl/isap.nsf/DocDetails.xsp?id=WDU20220001225> [accessed: 2.04.2026].
- Pastukh, O., Zhivotov, D., Vaitens, A., & Yablonskii, L. (2021). The use of modern polymer materials and wood in the construction of buildings in the form of geodesic domes. In *E3S Web of Conferences* (Vol. 274, p. 01024). EDP Sciences. <https://doi.org/10.1051/e3sconf/202127401024>
- Peng, Z. (2016). *Geodesic dome structural analysis and design* (Master's thesis). University of Southern Queensland. <https://sear.unisq.edu.au/id/eprint/31457>
- Peseke, H., Raso, R. V., Grohmann, M., & Bollinger, K. (2015). *Reflection about the first dome of Jena*. In *Proceedings of IASS Annual Symposia* (Vol. 2015, No. 18, pp. 1–15). International Association for Shell and Spatial Structures (IASS). <https://www.ingentaconnect.com/content/iass/piass/2015/00002015/00000018/art00010#> [accessed: 2.04.2026].
- Polski Komitet Normalizacyjny [PKN]. (2004a). *Eurokod 1. Oddziaływania ogólne [Eurocode. Basis of structural design]* (PN-EN 1990:2004).
- Polski Komitet Normalizacyjny [PKN]. (2004b). *Eurokod 1. Oddziaływania ogólne. Część 1-1: Ciężar objętościowy, ciężar własny, obciążenia użytkowe w budynkach [Eurocode 1: Actions on structures. Part 1-1: Densities, self-weight and imposed loads]* (PN-EN 1991-1-1).
- Polski Komitet Normalizacyjny [PKN]. (2005a). *Eurokod 1. Oddziaływania ogólne. Część 1-3: Obciążenie śniegiem [Eurocode 1: Actions on structures. Part 1-3: Snow loads]* (PN-EN 1991-1-3).
- Polski Komitet Normalizacyjny [PKN]. (2005b). *Eurokod 1. Oddziaływania ogólne. Część 1-4: Oddziaływania wiatru [Eurocode 1: Actions on structures. Part 1-4: Wind actions]* (PN-EN 1991-1-4).

- Polski Komitet Normalizacyjny [PKN]. (2006a). *Eurokod 3. Zasady projektowania konstrukcji stalowych. Część 1-1: Reguły ogólne i reguły dla budynków [Eurocode 3: Design of steel structures. Part 1-1: General rules and rules for buildings] (PN-EN 1993-1-1)*.
- Polski Komitet Normalizacyjny [PKN]. (2006b). *Załącznik krajowy do normy PN-EN 1993-1-1: Projektowanie konstrukcji stalowych. Część 1-1: Reguły ogólne i reguły dla budynków [National Annex to PN-EN 1993-1-1: Design of steel structures. General rules and rules for buildings] (PN-EN 1993-1-1/NA)*.
- Ramaswamy, G. S., Eekhout, M., & Suresh, G. R. (2002). *Analysis, design and construction of steel space frames*. Thomas Telford.
- Sadowski, K. (2020). Konstrukcje magnetyczne jako kontynuacja wizji architektury efemerycznej Richarda Buckminstera Fullera. *Architecturae et Artibus*, 12(3). <https://doi.org/10.24427/aea-2020-vol12-no3-02>
- Shrivastava, A., & Pendharkar, U. (2021). Study of optimised sectional shape for geodesic domes. *Journal of Xi'an University of Architecture & Technology*, 13(1), 407–411.
- Szmit, R. (2017). Geometry design and structural analysis of steel single-layer geodesic domes. In *Proceedings of the 2017 Baltic Geodetic Congress (BGC Geomatics)* (pp. 205–209). IEEE. <https://doi.org/10.1109/BGC.Geomatics.2017.9>
- Talashlioglu, T. (2019). A unified optimal design approach for geometrically nonlinear skeletal dome structures. *Periodica Polytechnica Civil Engineering*, 63(2), 518–540. <https://doi.org/10.3311/PPci.13329>

## WPLYW CZĘSTOTLIWOŚCI PODZIAŁU ORAZ BRYŁY PODSTAWOWEJ NA EFEKTYWNOŚĆ KONSTRUKCYJNĄ JEDNOWARSTWOWYCH STALOWYCH KOPUŁ GEODEZYJNYCH

### STRESZCZENIE

W niniejszym artykule przedstawiono porównawczą analizę numeryczną jednowarstwowego kopuły geodezyjnej o średnicy 30 m, opartych na dwudziestościanie foremny i ośmiościanie foremny. Przeanalizowano częstotliwości podziału 2 V, 4 V, 8 V i 16 V przy użyciu siatki klasy I. W badaniu przyjęto założenie, że zwiększenie częstotliwości podziału poprawia właściwości konstrukcyjne, a wybór bryły podstawowej wpływa na efektywność materiałową. Wyniki pokazują, że wyższe częstotliwości zmniejszają momenty zginające i przesuwają zachowanie konstrukcji w kierunku sił osiowych, co umożliwia zastosowanie mniejszych przekrojów i zmniejszenie masy. Przy częstotliwości 16 V kopuła dwudziestościana była o około 20% lżejsza od kopuły ośmiościennej. Kopuły oparte na dwudziestościanie wymagały również mniejszej liczby unikalnych długości elementów i osiągały lepszą wydajność geometryczną.

**Słowa kluczowe:** kopuła geodezyjna, częstotliwość podziału, dwudziestościan, ośmiościan, efektywność strukturalna, modelowanie parametryczne